

Evaluation and Suppression of Overrun of Microorganisms using Dynamics Model for Microrobotic Application

Naoko Ogawa^a Hiromasa Oku^a Koichi Hashimoto^{b,c} Masatoshi Ishikawa^a

^a *University of Tokyo, Japan*

^b *Tohoku University, Japan*

^c *PRESTO, JST, Japan*

Abstract. Our goal is to utilize living microorganisms as smart, autonomous microrobots. In previous work, we constructed a dynamics model of Paramecium cells for navigation using galvanotaxis (locomotion response to an applied electric field). In this paper, an overrun phenomenon, which affects the control performance, is evaluated using the proposed dynamics model, and it is found that the turning trajectory is independent of the individual ciliary forces. A trapping experiment based on this model is performed and better performance is achieved. This is an important step toward our eventual goal of using living cells as autonomous microrobots.

Keywords. Microrobot, Paramecium, Galvanotaxis, Model, Overrun, Trapping

1. Introduction

Today, there is great deal of interest in the measurement and control of objects at the micrometer and nanometer scales. Conventional technologies, however, have required human operators with good dexterity, a high level of expertise, and long experience. There is therefore a need for intelligent, autonomous microsystems to assist less skilled operators. However, there remain many problems to be solved before the practical implementation of such microsystems becomes realistic.

Our approach to overcome these problems is to utilize microorganisms [1]. Motile microorganisms have acquired sophisticated sensors and actuators for survival through the course of their evolution. In this sense, microorganisms are smart microrobots with complete autonomy. If we can develop techniques to control them freely by exploiting their intrinsic functions and behavior, we can realize multi-purpose, programmable, organic microrobotic systems that are superior to existing micromachine systems. By controlling microorganisms in this manner, we aim to achieve various applications, such as cell manipulation, microscopic transportation, smart microsensors, and assembly of micro-electro mechanical systems (MEMS).

One key technology to developing such microrobotic applications is navigation of cells and microorganisms. A promising candidate for navigation is to make use of gal-

vanotaxis, an intrinsic locomotor response to an electrical stimulus, because of its non-invasive and non-contact nature. Some recent studies successfully used galvanotaxis to achieve simple motion control of *Paramecium caudatum*, a kind of protozoa exhibiting strong galvanotaxis [1–3]. In these studies, however, the motion of the microorganisms was based on simple empirical models, and limited control performance was achieved. For instance, in turning of a cell, there was a considerable time lag of several hundred milliseconds, causing the cell to go too far, which we call the “overrun” phenomenon [1, 3]. To realize more precise control, it is essential to deal with *Paramecium* in the framework of standard robotics. Thus, as an essential first step, we constructed a dynamics model of *Paramecium* galvanotaxis using a bottom-up approach [4].

In this paper, we apply our previously proposed model to the suppression of overrun phenomena in order to improve the performance. We evaluated the overrun phenomenon using this model and found the interesting property that overrun is independent of the ciliary force, which allows us to easily implement countermeasures against overrun. Preliminary experiments based on this finding demonstrate better performance in trapping a cell within a small region. We expect that this technique will be effective toward our eventual goal of using living cells as autonomous microrobots.

2. Dynamics Model of *Paramecium* Galvanotaxis

In this section, we briefly describe the dynamics model of *Paramecium* galvanotaxis. More details and its evaluations are available in our previous work [4].

2.1. *Paramecium* and Its Galvanotaxis

Paramecium caudatum is a unicellular protozoan with an ellipsoidal shape, inhabiting freshwater. It swims by waving cilia on its body; thousands of cilia beat the water backward to yield forward propulsion by means of a reaction force [5]. The cilia therefore act as tiny actuators.

For navigation, we adopt galvanotaxis. *Paramecium* cells exhibit quite strong negative galvanotaxis [6]. An external electrical stimulus modifies the membrane potential and alters the ciliary movements, thus affecting the cell motion. Viewed macroscopically, the cell is made to swim toward the cathode in a DC electric field.

A *Paramecium* cell in an electric field shows a characteristic ciliary movement pattern. To analyze this movement, we assume an imaginary plane that is perpendicular to the electric field and located near the center of the cell, slightly closer to the cathodal end, dividing the cell into two parts, as illustrated in Figure 1. The electric field causes cilia on the anodal end to beat more frequently (ciliary augmentation) [7] and the cilia on the cathodal end to also beat more frequently but in the opposite direction (ciliary reversal) [8]. The asymmetry of the ciliary beatings generates a rotational force that orients the cell toward the cathode.

In order to analyze this phenomenon quantitatively, we constructed a dynamics model of *Paramecium* galvanotaxis, which is described below.

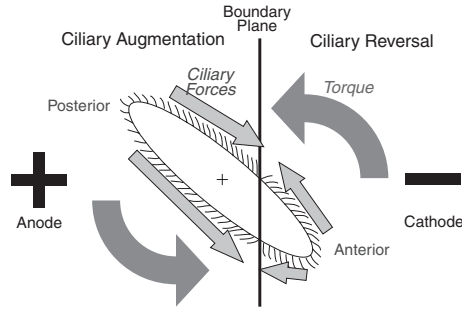


Figure 1. Qualitative explanation of galvanotaxis.

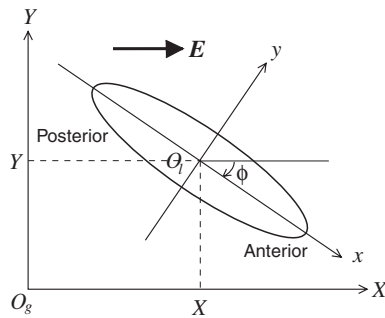


Figure 2. The global coordinate system (X, Y) .

2.2. Assumptions

By making several assumptions focusing only on those properties that are essential and dominant in galvanotaxis [4], we can describe the cell motion in a two-dimensional plane including the cell axis and the electric field vector. Hereafter, we consider cell motion only in this plane. Also, we can consider the cell as a two-dimensional ellipsoid on this plane.

We define a global coordinate system (X, Y) on the plane, as shown in Figure 2. It is fixed with respect to the external world, with the X -axis parallel to the electric field \mathbf{E} . Let ϕ be the angle of the cell axis in the global coordinate system ($\phi < 0$ in Figure 2, for the sake of convenience in deriving the model).

Let the cell shape be an ellipsoid \mathcal{E} with a major axis of length $2L$ and a minor axis of length $2R$. We assume that cilia are distributed uniformly around the edge of the ellipsoid with linear density n . In the presence of an electric field, imagine a plane perpendicular to the field (hereinafter referred to as “a boundary plane”). The shortest distance between the plane and the center of the cell is set to l .

The propulsion force yielded by one cilium is assumed to be f_0 in the absence of an electric field. In the presence of an electric field E , the force increases to $f = (1 + \beta E)f_0$, where β is a positive parameter.

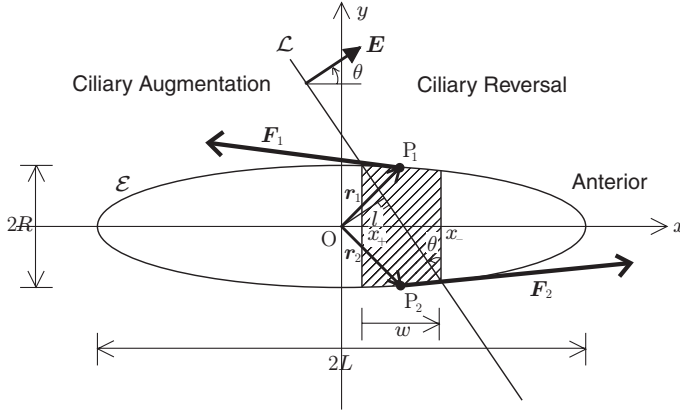


Figure 3. Parameters in the local coordinate system.

2.3. Model of the Torque

The Paramecium cell swims toward the cathode due to a torque caused by asymmetry of ciliary motion. In this section, we estimate this torque. First, consider an ellipsoid \mathcal{E} in the local coordinate system (x, y) , as illustrated in Figure 3. The asymmetry of ciliary beating exists only at the substantially trapezoidal region formed by the intersection of the boundary plane and the ellipsoid (shown as the hatched region in Figure 3). Thus, we have only to consider the forces generated at this region.

Because it would be too complicated to consider the individual minute forces generated by each cilium, here we focus on the resultant forces for simplicity. We set sites of action, P_1 and P_2 , at the midpoints of the sides of the trapezoid and assume the directions of the forces to be tangential to the ellipsoid. We then define position vectors, $\mathbf{r}_1 = \overrightarrow{OP_1}$ and $\mathbf{r}_2 = \overrightarrow{OP_2}$. Next, let us suppose that the magnitude of the resultant force is proportional to the “height” of the trapezoid w , which is a signed value the same sign as θ . Then, the propelling forces \mathbf{F}_1 and \mathbf{F}_2 at the points P_1 and P_2 , respectively, are represented by $\mathbf{F}_{\{1,2\}} = \mp fwn\mathbf{m}_{\{1,2\}}$, where \mathbf{m}_1 and \mathbf{m}_2 are the unit tangent vectors at P_1 and P_2 , and the \mp symbol indicates the two directions of ciliary beating. Thus, we find the torques at the points $P_{\{1,2\}}$, namely, $\boldsymbol{\tau}_{\{1,2\}} = \mathbf{r}_{\{1,2\}} \times \mathbf{F}_{\{1,2\}}$. It should be noted that these vectors are treated as three-dimensional in calculating cross products. The total torque rotating the cell body is given by $\boldsymbol{\tau} = \boldsymbol{\tau}_1 + \boldsymbol{\tau}_2$. Since its x and y components are obviously zero, hereafter we call its z component, τ_z , the “torque”.

Finally, the torque generated in the Paramecium cell oriented at angle ϕ is described as:

$$\tau_z(\phi) = -\frac{4LR^2 fns\sqrt{L^2c^2 + R^2s^2 - l^2}}{\sqrt{L^4c^4 + 2L^2R^2c^2s^2 + R^4s^4 - L^2l^2c^2 + R^2l^2c^2}}, \quad (1)$$

where $s = \sin \phi$ and $c = \cos \phi$.

2.4. Equations of Motion of Paramecium Cell

Using the torque estimated in the previous section, we now discuss the equations of motion of a Paramecium cell. In a micrometer-scale world, the inertial resistance of the

fluid is small enough to be negligible, and the viscous resistance becomes dominant instead. Hence we can apply Stokes' law.

Since a rigorous evaluation of the viscous resistance around an ellipsoid is quite complicated, here we approximate the viscosity by substituting Stokes' law for a sphere. Thus, the equation of motion for the translational motion of the cell can be approximated by $M\ddot{\mathbf{X}} + D\dot{\mathbf{X}} = \mathbf{F}$, where $\mathbf{X} = (X, Y)^t$ is the cell position, $\mathbf{F} = 2fn|x_a|e_{\mathbf{X}}$ is a forward propulsive force, $e_{\mathbf{X}} = (\cos \phi, \sin \phi)^t$ is a unit vector along the longitudinal axis, $D = 6\pi\mu R$ is the viscous friction coefficient, $M = \rho V$ is the cell mass, ρ is the cell density, and $V = 4\pi LR^2/3$ is the cell volume.

In addition, the equation of motion for the rotation is given by $I\ddot{\phi} + D'\dot{\phi} = \tau_z(\phi)$, where $I = \pi M(R^2 + L^2)/5$ is the moment of inertia for an ellipsoid, $D' = \delta\pi\mu L^3$ is the viscous friction coefficient, and δ is a coefficient to compensate for errors in the model.

Finally, integration of the equations of motion for the translational motion and the rotational motion leads to the following equations:

$$\dot{\mathbf{y}} = \mathbf{A}\mathbf{y} + \mathbf{B}(\mathbf{y}), \quad (2)$$

$$\mathbf{A} = \begin{pmatrix} 0 & 0 & 1 & 0 & 0 & 0 \\ 0 & 0 & 0 & 1 & 0 & 0 \\ 0 & 0 & -D/M & 0 & 0 & 0 \\ 0 & 0 & 0 & -D/M & 0 & 0 \\ 0 & 0 & 0 & 0 & 0 & 1 \\ 0 & 0 & 0 & 0 & 0 & -D'/I \end{pmatrix}, \quad \mathbf{B}(\mathbf{y}) = \begin{pmatrix} 0 \\ 0 \\ (P \cos \phi)/M \\ (P \sin \phi)/M \\ 0 \\ \tau_z(\phi)/I \end{pmatrix},$$

where $\mathbf{y} = (X, Y, \dot{X}, \dot{Y}, \phi, \dot{\phi})^t$ and $P = 2fn|x_a|$.

With parameters determined by experimental data, numerical experiments using our model demonstrated realistic behaviors, such as U-turn motions, like those of real cells. The validity of the model was also verified by comparing it quantitatively with experimental data, where the simulated data was approximately in agreement with several experimental results. See the previous work [4] for more details.

3. Evaluation of Overrun

3.1. Overrun in Paramecium U-Turn

We have reported several experiments of motion control of Paramecium cells, such as zig-zag motion, U-turn motion, and trapping cells within a small region [1]. However, these studies revealed the problem that it can take hundreds or thousands of milliseconds between applying the stimulus to turn the cell and completion of the actual turn [9]. This time delay resulted in poor performance; for example, cells overran out of the trapping region by a substantial distance [1]. In this paper we attempt to improve the performance by considering overrun in our proposed model.

The overrun is, in brief, a phenomenon that the cell goes too far in U-turn motion. Figure 4 illustrates a schematic overview of a U-turn of a Paramecium cell by reversal of the electrical stimulus. The cell does not turn only at the point of stimulus application (at P), but turns after a substantial overrun (at Q). Thus, let us define the *X-overrun* as the distance traveled in overshooting from P (stimulus point) to Q (turn point) in the

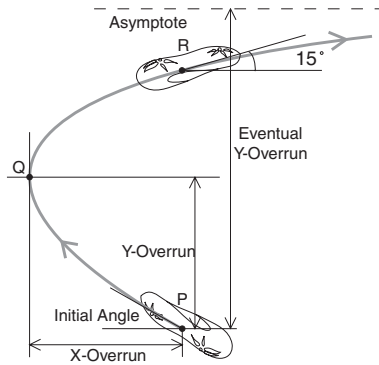


Figure 4. Definition of overrun.

X -direction (parallel to the electric field). Correspondingly, Y -overrun is defined as the distance from P to Q in the Y -direction.

3.2. Evaluation of Overrun

In order to evaluate the overrun using the proposed model, we performed numerical calculations. Numerical analysis software (MATLAB 7, MathWorks) was used for these calculations.

In numerical simulation, swimming cells encountered a stimulus reversal when they oriented at 30° with respect to the electric field ($\phi = -150^\circ$) at the point P. The X and Y distances between P and Q (the tip of the U-turn) were calculated to be referred as the X -overrun and the Y -overrun. Parameters were set based on several experimental results, as described in our previous work [1]. The force generated by cilia, f_{0n} , cannot easily be determined due to diversity among cells and the difficulty of precise measurement. However, it is possible to obtain a rough estimate based on actual measurements. Therefore, we used eleven types of values for f_{0n} with a suitable range, namely, from $0.5 \mu\text{N/m}$ to $1.5 \mu\text{N/m}$, in order to compare the results obtained.

Figure 5 shows time sequences in the X -direction for several values of f_{0n} . The minima of the curves correspond to the X -overrun. It is noteworthy that the X -distance to the point Q seems constant, whereas the time to arrive at Q varies depending on the ciliary force f_{0n} . In addition, the magnitude of the overrun agrees well with actual measurements [1].

Likewise, Y -overrun was also evaluated. The time sequence in the Y -direction for several f_{0n} is shown in Figure 6. The point where the inclination of the curve temporarily goes to zero represents the Y -overrun. Like the X -overrun, the Y -overrun is independent of the ciliary force f_{0n} . The terminal points of the curves indicate that the asymptotes and the eventual Y -overrun are almost constant, whereas the U-turn times depend on the ciliary force f_{0n} .

3.3. Evaluation of Whole Trajectory

These results indicate that the overruns for both the X and Y directions can be treated as constant, that is, independent of the ciliary force. Consequently, this leads to the natural hypothesis that the whole trajectory itself is independent of the ciliary force. We verified

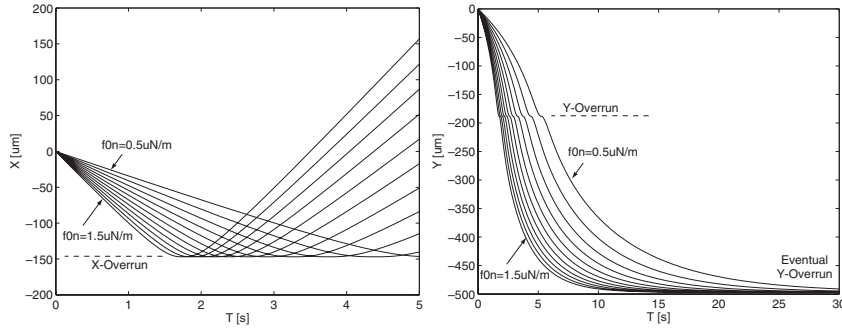


Figure 5. Time sequences of X positions for various $f_0 n$. **Figure 6.** Time sequences of Y positions for various $f_0 n$.

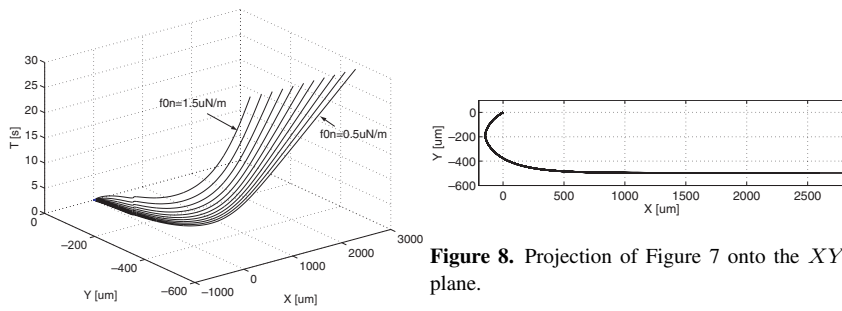


Figure 7. Relations among X -position, Y -position, and time t .

Figure 8. Projection of Figure 7 onto the XY plane.

this hypothesis by numerical calculations. Figure 7 shows the relationships among the X -position, Y -position, and the time t in the three-dimensional space, which are extracted from Figure 5 and Figure 6. Its projection onto the X - Y plane is shown in Figure 8 to show multiple trajectories overlaid. The trajectories are completely identical, suggesting that the whole trajectory is independent of the ciliary force.

These experiments imply that, at least for the U-turn motion, disparities in the ciliary force have little or no influence on the cell trajectory. This is a quite convenient property for motion control of Paramecia for the following reasons. First, it is unnecessary to consider the ciliary force in dealing with only positions of cells. This is beneficial because the experimental identification of ciliary motion is quite difficult. Second, disregarding individual diversity in the ciliary forces allows us to apply a-priori countermeasures against the overrun phenomenon without performing calibration in advance. Finally, it will allow for simple trajectory planning and control of Paramecium cells in future works.

4. Trapping Experiment Considering Overrun

The discussion in the previous section suggested that we can improve the performance a-priori without detailed knowledge of the cell properties. In this section, this finding

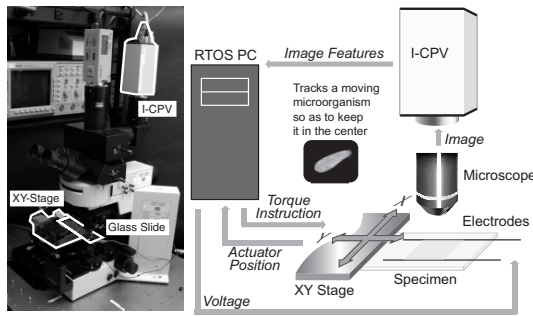


Figure 9. System configuration.

is applied to a trapping experiment. Note that this is a preliminary experiment for more rigorous evaluation to be forthcoming.

4.1. Experimental Setup

This section briefly describes the experimental setup. For more details, see our previous work [1].

The configuration of the overall system is illustrated in Figure 9. An electrical stimulus is applied to cells swimming in a chamber mounted on an XY stage. The stage is controlled by a high-speed vision system called I-CPV to keep a cell in the center of the field of view. Using reading encoders on the stage and performing coordinate transformation, we can obtain the global position of the cell.

The I-CPV system [10] integrates an image intensifier with a Column Parallel Vision (CPV) system, which is a high-speed vision system developed for robotic applications [11]. It captures and processes 8-bit gray-scale images with 128×128 pixels at 1-kHz frame rate. Each pixel has a programmable general-purpose processing element (PE) based on the S^3PE architecture [12]. The I-CPV is mounted on an upright optical microscope (Olympus, BX50WI) and captures dark-field images. From the captured images, the I-CPV system provides the image moments every 1 ms. The trajectory and orientation of the target are reconstructed from the moments and are used for visual feedback control of the XY stage (SMC, LAL00-X070) to achieve “lock-on” tracking of moving microorganisms [13].

4.2. Methods and Materials

The system can adjust the stimulus voltage applied to the electrodes according to the cell status captured by the I-CPV system. For example, the system can reverse the voltage when a cell goes out of a certain region, which causes the cell to move in the opposite direction. This allows us to trap the cell within the region. We adopt this simple closed-loop trapping experiment as a preliminary demonstration.

The stimulus was adjusted in real time according to the target status. The width of the trapping region was set to 1 mm. The electrical stimulus was applied in the X direction by two carbon electrodes on either side of the chamber. The strength of the voltage gradient was 4.1 V/cm.

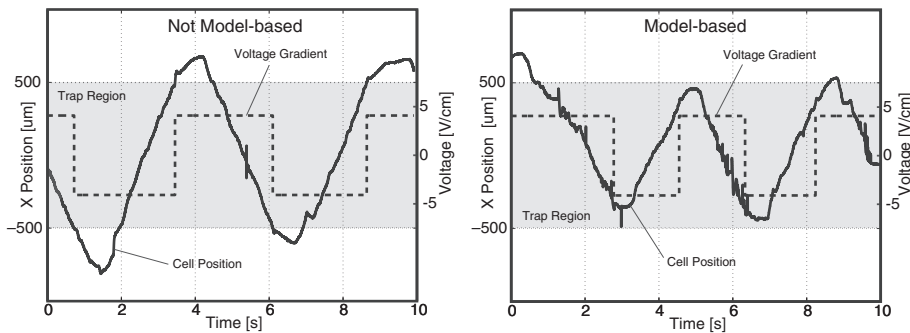


Figure 10. Applied voltage (dashed lines) and X position (parallel to the electric field) of a cell (solid lines). The shaded region is the bounded region for trapping. Left: conventional method in which overrun was ignored [1]. Right: proposed method in which overrun was accounted for. Overrun was suppressed in the proposed method and better trapping performance was achieved.

In previous experiments, the electrical stimulus was reversed just when the cell moved outside the boundaries. This time, however, we embedded the overrun estimates of $140\ \mu\text{m}$ derived from the numerical calculations shown in Figure 5 into the system; the system was designed to reverse the stimulus before the boundary lines with the undershoot of $140\ \mu\text{m}$ equal to the estimated overrun so that the cell would turn just at the boundaries.

Wild-type *Paramecium caudatum* cells were cultured at $20\text{--}25^\circ\text{C}$ in a soy flour solution. Cells grown to the logarithmic or stationary phase (4–10 days after incubation) were collected together with the solution, filtered through a nylon mesh to remove debris, and infused into the chamber.

4.3. Results

Figure 10 shows time sequences of the electrical stimulus (dashed lines) and cell position in X -direction (solid lines). The shaded region is the bounded region for trapping. Comparing the case in which overrun is considered (right) and the case where it is not considered (left), it is clear that overrun was suppressed with the proposed method, implying that the trapping performance was improved. Note that this result is preliminary and further evaluation needs to be performed. Particularly, more rigorous experiments and evaluation are to be performed by obtaining three-dimensional data from our tracking and focusing system [13, 14]. In addition, we are planning to evaluate statistic properties of overrun by several cells under various conditions.

5. Summary

In this paper, we evaluated the overrun of *Paramecium* cells in galvanotactic navigation and found that the trajectory is independent of ciliary force. Using this finding, we improved the performance of a trapping task. This is an important step towards using living cells as microrobots.

References

- [1] N. Ogawa, H. Oku, K. Hashimoto and M. Ishikawa. Microrobotic visual control of motile cells using high-speed tracking system. *IEEE Trans. Robotics*, **21**(4), 704–712, Aug. 2005.
- [2] R. S. Fearing. Control of a micro-organism as a prototype micro-robot. *2nd Int. Symp. Micromachines and Human Sciences*, Oct. 1991.
- [3] A. Itoh. Motion control of protozoa for bio MEMS. *IEEE/ASME Trans. Mechatronics*, **5**(2), 181–188, June 2000.
- [4] N. Ogawa, H. Oku, K. Hashimoto and M. Ishikawa. Dynamics model of Paramecium galvanotaxis for microrobotic application. *Proc. 2005 IEEE Int. Conf. Robotics & Automation (ICRA 2005)*, 1258–1263, Apr. 2005.
- [5] Y. Naitoh and K. Sugino. Ciliary movement and its control in *Paramecium*. *J. Protozool.*, **31**(1), 31–40, 1984.
- [6] H. Machemer and J. de Peyer. Swimming sensory cells: electrical membrane parameters, receptor properties and motor control in ciliated Protozoa. *Ver. Deut. Zool. gesell.*, 86–110, 1977.
- [7] T. Kamada. Control of galvanotropism in Paramecium. *J. Fac. Sci. Imp. Univ. Tokyo, Sect. IV, Zoology*, **2**, 123–139, 1929.
- [8] K. Ludloff. Untersuchungen über den Galvanotropismus. *Arch. Ges. Physiol.*, **59**, 525–554, 1895.
- [9] N. Ogawa, H. Oku, K. Hashimoto and M. Ishikawa. Response measurement of Paramecia for realization of organized bio-modules. *Proc. 2003 JSME Conf. Robotics and Mechatronics (Robomec'03)*, 2P2–3F–E3, May 2003. in Japanese.
- [10] H. Toyoda, N. Mukohzaka, K. Nakamura, M. Takumi, S. Mizuno and M. Ishikawa. 1ms column-parallel vision system coupled with an image intensifier; I-CPV. *Proc. Symp. High Speed Photography and Photonics 2001*, **5-1**, 89–92, 2001. in Japanese.
- [11] Y. Nakabo, M. Ishikawa, H. Toyoda and S. Mizuno. 1ms column parallel vision system and it's application of high speed target tracking. *Proc. 2000 IEEE Int. Conf. Robotics & Automation (ICRA2000)*, 650–655, Apr. 2000.
- [12] M. Ishikawa, K. Ogawa, T. Komuro and I. Ishii. A CMOS vision chip with SIMD processing element array for 1 ms image processing. *Dig. Tech. Papers of 1999 IEEE Int. Solid-State Circuit Conf. (ISSCC'99)*, 206–207, 1999.
- [13] H. Oku, N. Ogawa, K. Hashimoto and M. Ishikawa. Two-dimensional tracking of a motile micro-organism allowing high-resolution observation with various imaging techniques. *Rev. Sci. Instr.*, **76**(3), Mar. 2005.
- [14] Theodorus, H. Oku, K. Hashimoto and M. Ishikawa. Optical axis tracking of microorganism using high-speed vision. *Proc. Focus on Microscopy 2005*, Mar. 2005.